High-Speed OH-PLIF Diagnostics of Flame Flashback in Low Swirl Hydrogen-Enriched Flames

Pradeep Parajuli[1, 2], Peter Strakey[1]

[1]National Energy Technology Laboratory, 3610 Collins Ferry Road, Morgantown, WV, 26505, USA

[2]NETL Support Contractor, 3610 Collins Ferry Road, Morgantown, WV, 26505, USA

ABSTRACT

This paper reports flashback events observed in hydrogen-enriched flames stabilized in a low swirl burner (LSB) at atmospheric pressure and temperature conditions. The fundamentals of hydrogen-rich stable flames and spatiotemporal investigation of flashback phenomena were observed experimentally using a high-repetition-rate nanosecond (ns)-duration hydroxyl radical planar laser-induced fluorescence (OH-PLIF) diagnostic. Testing was conducted in an optically accessible pre-mixing section of a LSB with inlet pre-mixing velocities ranging from 5 to 10 m/s for methane and hydrogen (50 – 90% by mole) blends. Swirlers with two different turning angles, 26^o and 33^o, and three different perforated plate hole diameters, 1.08, 1.12 and 1.16 mm, with measured swirl numbers varying from 0.43 to 0.49 were used in this study at atmospheric temperature and pressure inlet conditions. The flashback propensity showed a dependence on the proximity of the lifted flame to the burner exit (termed as lift-off length, L) which was dependent on the pre-mixer velocity (V), hydrogen content (X_{H_2}) and equivalence ratio (ϕ) at constant temperature and pressure conditions. High-speed OH-PLIF images revealed lifted flames were first observed at low ϕ/ X_{H_2} condition which then changed to a M-shaped flame attached to burner rim with the increase in ϕ/ X_{H_2}. Further increases in ϕ/X_{H_2}, depending upon other inlet parameters, triggered flame flashback into the pre-mixing section. Flashback occurred when burning began in the outer shear layer and the leading flame brush propagated into the nozzle. Such spatiotemporally resolved high-speed OH-PLIF imaging provides insights on different stages of flashback in a LSB – flashback initiation, transition of flame propagation from burner exit to the swirler and flashback to flame holding transition. Flame ϕ at flashback showed an expected linearly increasing trend with increasing V and decreasing X_{H_2} and the conclusions drawn aligned well with detailed investigations. For identical inlet conditions, flashback propensity decreased with increasing perforated-plate hole diameter and increasing swirler vane angle.

INTRODUCTION

Hydrogen and hydrogen-enriched fuels are considered a clean and sustainable energy source and are the key enabler of the energy transition to replace conventional fuels for the development of next-generation gas turbine engines [1-4]. The use of hydrogen-enriched fuels can significantly reduce the production of carbon-based products in the power generation industry. However, high-hydrogen flames are particularly susceptible to flashback which is one of the key issues in retrofitting lean-premixed natural gas turbine combustors. Flashback events occur when the flame front propagates upstream from the combustor into the premixer section. Such events can cause catastrophic failure of the combustor as the pre-mixing tubes are not designed to handle a high heat load. The propensity for flashback increases with increasing in hydrogen content of the reactant mixture due to the faster chemical kinetics and smaller quenching lengths of hydrogen-rich flames [5].

The successful design of next-generation gas turbine engine combustors requires a better fundamental understanding of flashback events. Currently, most gas turbine combustors include a swirling flow for flame stabilization and mixing processes which requires a detailed study of flashback events. Swirl-stabilized flame methods are essential to lean-premixed combustion systems because of their significant benefits such as an increase in flame intensity and stability, as well as combustor performance [6]. Low swirl burners (LSBs) have gained increasing attention since they were originally developed by Cheng [7] for fundamental studies. LSBs have a non-swirling core surrounded by a swirling shroud and utilize a flow divergence concept allowing the flame to freely propagate and stabilize at a position where

the local flow velocity is equal and opposite to the flame speed [8]. Flashback becomes likely to occur if the bulk flow velocity is reduced further as the velocity at the burner exit is close to the flame speed. Avoidance of such flashback events is critical to the design of hydrogen-safe gas turbine combustors; however, the lack of relevant fundamental knowledge of flashback modes in LSBs and their underlying mechanism remains a major obstacle.

In this study, the flashback mechanism in low swirl flames is investigated in an optically accessible LSB via the visualization of spatiotemporally resolved hydroxyl (OH) radicals using Planar Laser-Induced Fluorescence (PLIF). This study is an extension of previous work conduced at the National Energy Technology Laboratory (NETL) [9]. In the next section, a brief description of the optically accessible LSB, high-speed pulsed laser, and detection system are presented. Section 3 presents a series of single-laser-shot OH-PLIF images recorded while the LSB is operated under flashback mode and provides some insights on flashback mechanisms. A detailed investigation of different inlet mixture parameters and varying swirler geometries on burner equivalence ratio at flashback are studied and outlined.

EXPERIMENTAL APPARATUS

The experimental setup used for these measurements consists of an optically accessible laboratory-scaled swirl-stabilized burner, a high-repetition rate ns-pulsed laser system, a high-speed detection system, and is displayed schematically in Fig. 1.

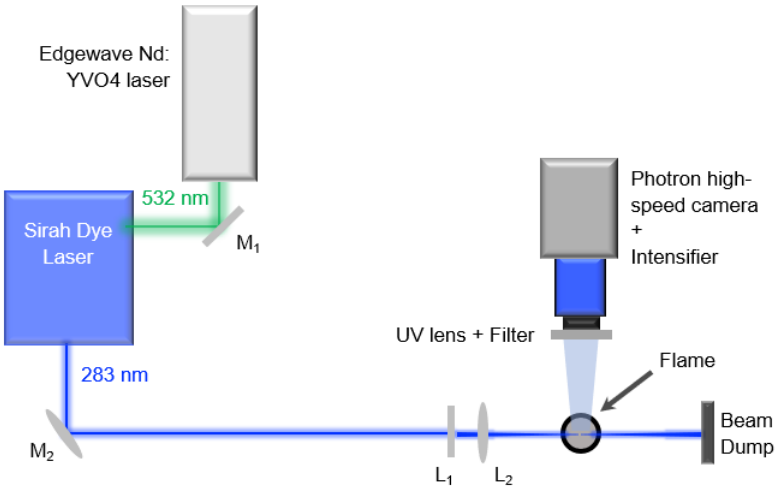

Figure 1: Schematic diagram of the experimental apparatus for OH-PLIF imaging in a LSB (M_1: 532 nm mirror; M_2: 284 nm mirror; L_1 & L_2: sheet-forming optics).

A. Burner Configuration

The burner facility consists of fuel (H_2 and CH_4) and air sources, mass flow controllers, flashback and flame management sensors and solenoid valves, a flow straightener, swirlers, and optically accessible pre-mixer assembly. A mixture of CH_4 gas with varied percentages of H_2 gas is premixed with air and is fed into a flow straightener to minimize the lateral velocity of the reactant mixture. The mixture then enters the swirler which serves to enhance flame stabilization. The burner system used in this study is the same as that used by Searle et al. [9] during previous flashback studies except the burner was modified to provide optical access in the pre-mixing section to visualize flashback dynamics. A 21.2-mm inner diameter and optically accessible pre-mixer assembly utilized in the present study is shown in Fig. 2a. The pre-mixer tube is sliced by a plane parallel to its axis to fit an optical window for laser sheet and imaging access. The optical window was fabricated using a clear fused quartz tube with a section cut out to fit into the pre-mixer tube. A thermocouple is inserted into the premixing section of the burner via a tiny port just above the swirler to detect the flashback when it occurs.

The swirler is the most important component of this burner and its design is depicted in Fig. 2b. The swirler was additively manufactured from 316 stainless steel using laser powder bed fusion. The air/fuel mixture through the central channel remains straight while that through the swirler vanes impart swirling motion to the annular flow

promoting flow divergence. A perforated plate is attached to the center channel which breaks down the large turbulent structures and balances the pressure drop across central and annular region. The more flow blocked by the central perforated region, the more flow that passes through the annular region of the swirler. The design dimensions for the swirler, perforated plate and optical window are provided in Table 1. Briefly, it has an injector radius of 10.4 mm, 16 curved swirler vanes of thickness 0.75 mm. The swirler angle, α, and perforated plates hole diameter, d, are varied to achieve measured swirl numbers between 0.43 to 0.49. Such a small range in swirl number is optimal to investigate LSB performance [8]. The radius ratio (R), defined by a ratio of center-body outer radius to injector radius is kept constant at 0.65. The perforated plate fitted to the swirler has 25 equal-sized holes (1.08, 1.12 and 1.16 mm in diameter) arranged in a circular grid to give 78.3, 76.7, and 75% blockage respectively, regulating the axial mass flow rate through the center channel. The swirler is recessed from the burner tube exit into the pre-mixer section by 27 mm and is essential to producing lift flames.

Table 1 Design parameters for swirler, perforated plate and optical window

Swirler	**Unit**	**Value**
Injector radius (R_i)	mm	10.4
Center-body outer radius (R_c)	mm	6.8
Radius ratio (R)	-	0.65
Center-body axial length (l_c)	mm	16
Center-body wall thickness (t_c)	mm	1
Swirler angle (α)	degree	26 and 33
Number of vanes (n)	-	16
Vane axial length (l_v)	mm	12
Vane thickness (t_v)	mm	0.75
Perforated plate	**Unit**	**Value**
Thickness (t)	mm	1
Hole diameter (d)	mm	1.08, 1.12 and 1.16
Number of holes (n_{holes})	-	25
Hole to burner diameter ($d/2R_i$)	-	0.058
Optical window	**Unit**	**Value**
Inner diameter (ID)	mm	22
Outer diameter (OD)	mm	25
Window length (l)	mm	63.5

B. Laser System and Imaging Apparatuses

The laser diagnostic system for the OH-PLIF imaging consists of a ns-duration Nd:YVO4 laser (INNOSLAB, Model: IS400-2-L) operating at 1,064-nm wavelength. The frequency-doubled laser beam at 532 nm wavelength with an input power of ~110 W at 20 kilohertz (kHz) and a unique 3 mm × 8 mm rectangular beam profile is used to pump a frequency-tunable dye laser (Sirah, Model: CREDO-DYE-N). The dye laser includes a high flow rate dye cell filled with a solution of rhodamine-6G dye diluted in pure ethanol which allows efficient production of a ~568 nm beam. The laser beam is frequency doubled in a nonlinear crystal to generate ultraviolet (UV) radiation near 284 nm and is isolated from the fundamental beam using a wavelength separation unit. The UV beam is guided into the probe region using a 45° mirror and a combination of cylindrical and spherical lenses to generate a beam sheet of approximately 30 mm height to excite the OH $A^2\Sigma^+$-$X^2\Pi$ (1,0) band. The OH-PLIF signal is collected perpendicular to the direction of the propagation of the laser beam sheet using a high-speed intensifier (Invisible Vision, Model: UVi 1850-10 S25) coupled to a high-speed CMOS camera (Photron, Model: FASTCAM SA-Z). An appropriate set of filters is mounted in front of the detection system to collect strong OH fluorescence emission near 309 nm and block unwanted chemiluminescence interference and laser scattering.

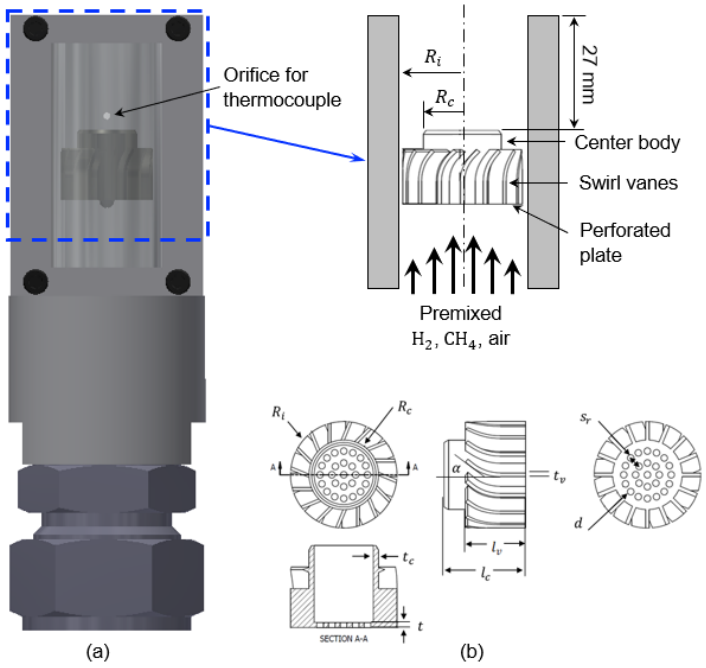

Figure 2: Design of (a) optically accessible pre-mixer system (b) swirler used in the present study.

RESULTS AND DISCUSSIONS

The burner was operated in two different configurations to characterize stable flames and flame flashback. The initial temperature and pressure of the gaseous mixture were set at 300 K and 1 atm, respectively. Before the test, the dependence of the OH-PLIF signal on the excitation wavelength was recorded in an atmospheric pressure 10%H_2/90%CH_4-air flame at ϕ = 0.7. The laser wavelength was scanned within the ±1-nm range around 283.5 nm, observing the OH-PLIF signal to find the peak excitation wavelength. As expected, the optimized excitation wavelength was found to be 283.9 nm, confirmed by the OH signal excitation spectrum obtained from LIFBASE [10]. Also, the OH-PLIF signal shows no apparent deviation from the expected linear dependence (owing to single-photon excitation) for the range of laser energy scanned, suggesting no saturation effect and hence the laser energy was held constant at ~ 0.05 mJ/pulse for the remaining experiments.

A. Characterization of Low Swirl Stabilized Flame

1. Effect of Inlet Pre-mixer Velocity

To investigate the high-hydrogen flame dynamics, the OH-PLIF images were recorded as a function of inlet pre-mixer velocity (V) at 20 kHz-repetition-rate. Velocity was varied from 5 to 10 m/s keeping ϕ and X_{H_2} constant at 0.4 and 70% respectively. Several spatiotemporally resolved, single-laser-shot OH-PLIF images were acquired and 500 such individual frames were averaged together to analyze lift-off length (L, distance from the burner rim to the base of the lifted flame) during post-processing. Lift-off length has a strong correlation to the flame stabilization and flashback mechanism and is an area of research for combustor designers and the combustion diagnostic community [11-14]. These freely propagating lifted flames produced by the LSB do not interact with the burner wall minimizing the heat transfer to the nozzle wall [15]. Figure 3 shows that L tends to increase linearly with V and this increase in L is driven by higher inlet velocities which push the combustion zone further downstream. Quantitatively, L increases from 1 mm above the burner to approximately 6 mm when the velocity is increased from 5.5 m/s to 10 m/s. A similar effect on gaseous fuel combustion with the jet velocity was observed experimentally and predicted computationally previously in the literature [13, 16-18]. This shows that as the local gas velocity is increased compared to the flame speed, the risk of flashback is minimized.

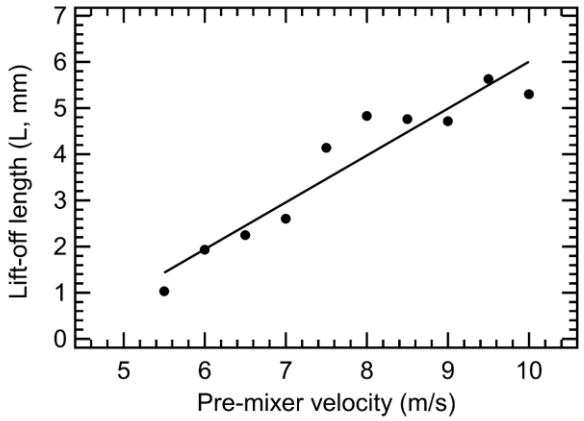

Figure 3: Variation of L as a function of V for 70%H_2/30%CH_4-air flame at ϕ = 0.4.

2. Effect of Hydrogen Content

Shown in Fig. 4 is the dependence of L on X_{H_2} in the reactant mixture. The ϕ and V were kept constant at 0.4 and 7.5 m/s, respectively. A detailed study of the effect of X_{H_2} on L revealed that increasing the X_{H_2} in the mixture tends to decrease L and increases the propensity of flashback in the hydrogen-enriched flames. When compared to the velocity, L in hydrogen-enriched flames is more sensitive to the X_{H_2} in the reactant mixture supporting the claim made by Liu et al. [13]. The decrease of L with increasing X_{H_2} was found to be nonlinear as L decreased faster at low X_{H_2}. A similar nonlinear decrease owing to the changes in autoignition delay time and flame speed was also observed by Liu et al. [13] during an OH* chemiluminescence study in hydrogen auto-ignited flames. A sudden rise in the calculated flame speed (S_L) is observed when X_{H_2} is increased above 70% in hydrogen-enriched flame as depicted in Fig. 5b. The change in flame shape occurred at high X_{H_2} which is strongly affected by burning in the outer recirculation zone that pulls the flame close to the burner exit increasing the flame flashback risk. It was observed that OH concentration increases at a higher X_{H_2} in the reactant mixture. The increase in OH concentration also relates to an increase in flame temperature which is expected as a hydrogen flame is hotter than a methane flame at the same ϕ. A similar effect of the X_{H_2} on OH signal was observed by Yang et al. [19] while investigating syngas/air-premixed turbulent flame combustion.

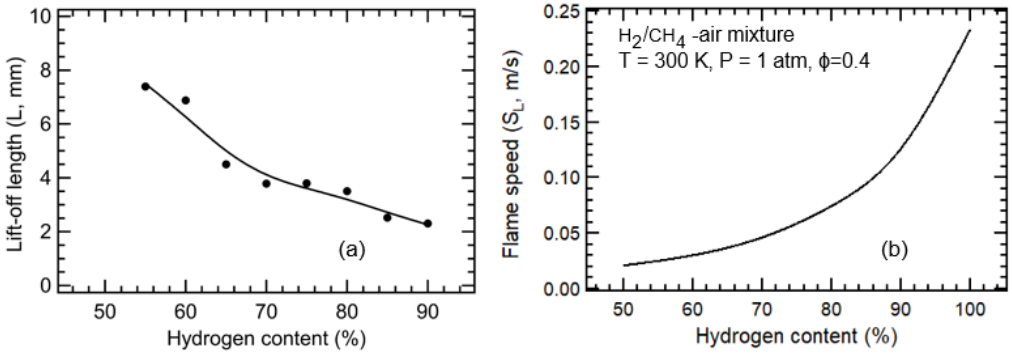

Figure 4: Variation of (a) L as a function of X_{H_2} in the reactant mixture at V= 7.5 m/s and ϕ = 0.4. (b) calculated S_L as a function of X_{H_2} in the reactant mixture at ϕ = 0.4.

3. Effect of Equivalence Ratio

The OH-PLIF diagnostic was applied to measure the experimental OH radical signal as a function of ϕ in a 70%H_2/30%CH_4-air flame. The X_{H_2} and V were kept constant at 70% and 10 m/s, respectively. The corresponding OH-PLIF dependency on ϕ is shown in Fig. 5a. The general trend is OH radical concentration peaks at a stoichiometric

condition and decays rapidly as the reactant mixture becomes leaner. A similar trend is observed experimentally where the OH-PLIF signal decays as ϕ is decreased from 0.60 to 0.35. In this study, ϕ was scanned in a narrow range of 0.35 to 0.60, limited by lean blowout condition and avoidance of flame flashback. The equilibrium temperature calculated using the STANJAN chemical equilibrium calculator is also included in the plot which shows an increase of approximately 500 K temperature when ϕ is increased from 0.35 to 0.60. Detailed study of ϕ on L revealed that increasing ϕ brings the flame closer to the burner surface increasing the risk of flashback due to increased flame speed. As ϕ is increased, the flames ultimately attach to the burner tube edge with uniform OH-intensity and local burning rates [6] and flashback then occurs once a threshold ϕ is reached. This decrease in L is evident in Fig. 6 when ϕ is increased from 0.40 (top row) to 0.55 (bottom row). Six single-laser-shot frames each for the two ϕs studied are presented here. The dark regions represent either the unburnt fuel-air reactants or surrounding air depending on the location, while the bright red and yellowish portion indicates the presence of hot combustion products. The light intensity of this portion has a direct relationship with OH radical concentration and the combustion intensity of the flame. It is observed that low OH radical concentration exists in the inner part of the flame zone. The flame front shows high OH concentration and is characterized by wrinkles especially in the top region and fluctuates from frame to frame. The increase in ϕ induced a higher turbulent flame speed and more dynamic features like wrinkling, flame breakages, and an increase in flame width as observed in Fig. 6.

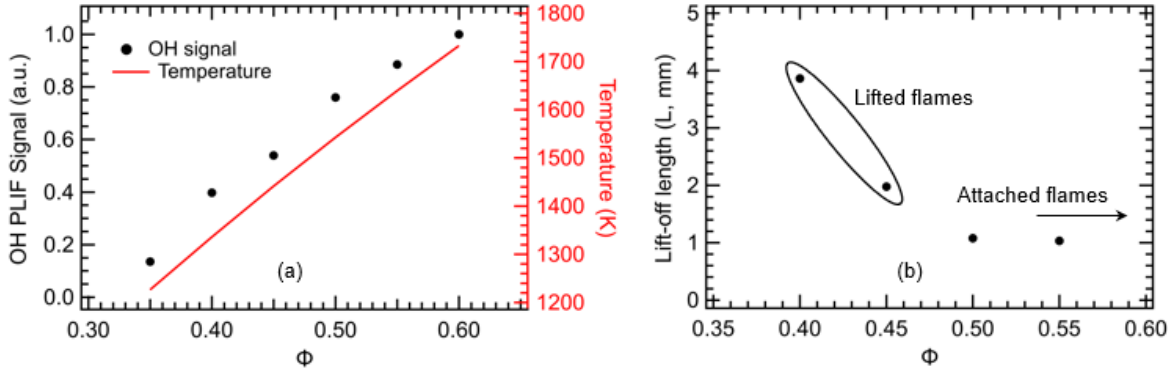

Figure 5: (a) Variation of OH-PLIF signal and equilibrium flame temperature as a function of ϕ for 70%H_2/30%CH_4-air flame at V = 10 m/s. (b) L as a function of ϕ for 70%H_2/30%CH_4-air flame at V = 7.5 m/s.

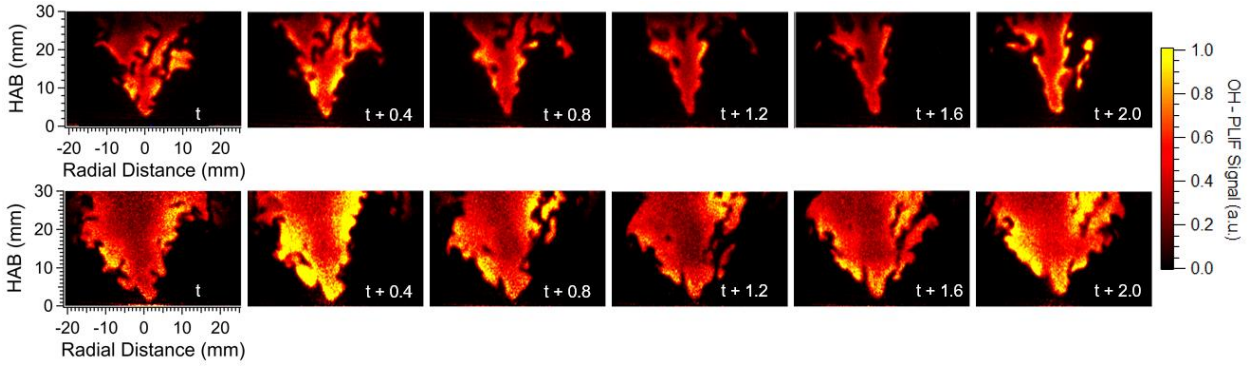

Figure 6: Sequence of single-laser shot OH-PLIF images showing flame dynamics for 70%H_2/30%CH_4-air flame at V of 7.5 m/s and ϕ = 0.4 (top row) and ϕ = 0.55 (bottom row). The time stamp for the occurrence of each event is shown on the bottom right corner of each frame in ms.

B. Investigation of Flame Flashback Events

In this section, the global propagation behavior of hydrogen-enriched low swirl flames and flashback to flame holding transition during flame flashback process are discussed. The flashback experiments were conducted for different fuel

compositions where the pre-mixer velocity through the mixing tube varied in the range of 5 to 10 m/s and the hydrogen content in the reactant mixture varied in the range of 50 to 90%. The swirler designs selected for this study have two swirling angles, 26° and 33°, and three different center-body hole diameters, 1.08, 1.12, and 1.16 mm with measured swirl numbers varying from 0.43 to 0.49. The atmosphere and pressure conditions at inlet were set at 300 K and 1 atm, respectively. During the flashback experiments, the burner was operated in a ramping mode by keeping V and X_{H_2} constant and increasing ϕ until the occurrence flashback (whenever applicable). The $\frac{d\phi}{dt}$ defined by the change in ϕ with respect to time, t was set at 0.001, i.e., for each 1-s time interval, ϕ was increased by 0.001 and was dictated via the mass flow controllers. A frame rate of 1 kHz with camera resolution of 512 × 512 or 1024 × 1024, which is equal to a field of view of 22 × 22 mm or 44 × 44 respectively was used.

1. Flashback Characterization in LSB

Figure 7a depicts the stable freely propagating lifted flame in LSB at low ϕ. A step increase in ϕ ignites the shear layer and a M-shaped flame attached to the burner rim is produced. A further increase in ϕ initiates the flame flashback process and the leading edge of the flame in the core of the flow ingresses within the pre-mixer tube (Fig. 7b). The flame rapidly propagates upstream into the pre-mixer tube within few "ms" and stabilizes itself on the rim of the center-body of the swirler in between the non-swirling core and the swirling annulus (Fig. 7c). Once stabilized, the flame doesn't propagate further upstream. A similar flashback process was observed for all range of X_{H_2} investigated during this study.

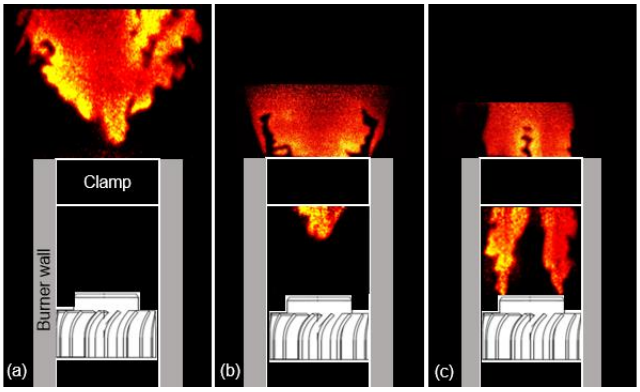

Figure 7: (a) Stable low swirl lifted flame (b) flashback initiation (c) flame holding post flashback occurrence

Flashback initiation:
The appearance of the flashback phenomenon occurring in this LSB configuration is depicted in Fig. 8. Interestingly, a sequence of three flame propagation phenomena was observed during the flashback investigation in this study. In the first phase, the flashback originates when the flame first penetrates the end of the mixing tube and the flame brush ingresses at the central part of the LSB into the center non-swirling region. Prior to flashback initiation, the flame exhibited a fluctuating behavior and flame instability was observed due to intermittent burning in the outer shear layer. The flame structures continue to interact strongly with the fresh unburnt reactant mixture flow around it and appear to rapidly grow in size within a few milliseconds. This leading edge of the flame continues to propagate upstream (indicated by white arrows) and this stage lasts for 50-60 ms.

Flame-flow interaction and flashback propagation:
Once the propagating flame structure approaches the swirler, it splits into two leading tips as indicated by white oval at t = 59 ms. At t = 60 ms, one can see that a leading tip of the flame shifts from the center non-swirling core to the inner shear layer. The flame structure extends further upstream along the shear layer that exists between non-swirling core and swirling annulus. From t = 60 ms to t = 63 ms, the visual evidence (red arrows) suggests that the shear layer facilitates the flame propagation upstream within the mixing tube until it reaches the rim of the center-body of the swirler.

Flame holding on the swirler:

Once a part of the propagating flame structure is attached to the rim at t = 64 ms, it ignites the incoming fresh mixture forming a conical flame stabilized on the rim of the center-body completely. It is likely that the ignition propagates along the inner shear layer within a few ms until the flame is anchored inside the mixing tube between the non-swirling core and swirling annulus. Once the flame is anchored, it doesn't propagate further upstream but continues to interact with fresh unburnt reactants, fluctuating from frame-to-frame. Several single-laser-shot OH-PLIF images were acquired visualizing the anchored flame and 200 such individual frames were averaged during post-processing and is depicted in bottom right corner of Fig. 8. The anchored flame is W-shaped in appearance with two flame fronts – inner and outer formed by non-swirling reactants and swirling reactants respectively. Potential explanations for the sustained flame anchoring in the mixing tube could be; 1) the continuous presence of fresh unburnt mixture inside the tube and 2) heating of the inner wall of the mixing tube and rim of the center-body reducing quenching distance.

Avoidance of flashback of high-hydrogen flames is critical to the design of hydrogen-safe gas turbine combustors and requires experimental observation of flashback mechanisms. Previous studies lack the experimental visualization of flashback to flame holding processes in LSBs. The mechanisms responsible for flashback are also not stated explicitly and are inconclusive in these studies and it is assumed that none of the standard flashback mechanisms like boundary layer, combustion instability and combustion induced vortex breakdown are solely responsible for flame flashback in the LSB. Studies suggest that flashback might originate in the region of high turbulent kinetic energy which occurs in the shear layers [20]. High-speed OH-PLIF images recorded during flashback initiation confirm the burning in the outer shear layer causing the flame to exhibit fluctuating behavior and instability. This effect can be seen when looking at the flame gap inside red ovals in Fig. 9 and as a consequence of this, the flame propagates upstream into the pre-mixer tube. The downward shift of the central part of the flame along the axis can also be seen in Fig. 9 (white arrows). Hence, shifting the down plane geometry to minimize the turbulence intensities might improve the flashback resistance in the LSB. It is also possible that thermo-diffusive instabilities might lead to an amplification of flame fluctuations which leads to upstream flame propagation into the nozzle [21, 22]. Once the flame enters into the pre-mixer tube, the upstream flame propagation is facilitated by the inner shear layer above the center-body wall between the swirled and unswirled flows. Studies suggest that these shearing motions possess the same turbulence intensities as that found in the outer shear layer which generate high vorticity that pulls the flame upstream [22, 23]. Therefore, minimizing the shear turbulence by tapering the trailing edge of the center-body wall or reducing the swirling angle to an optimum level can help address flashback issues via the inner shear layer.

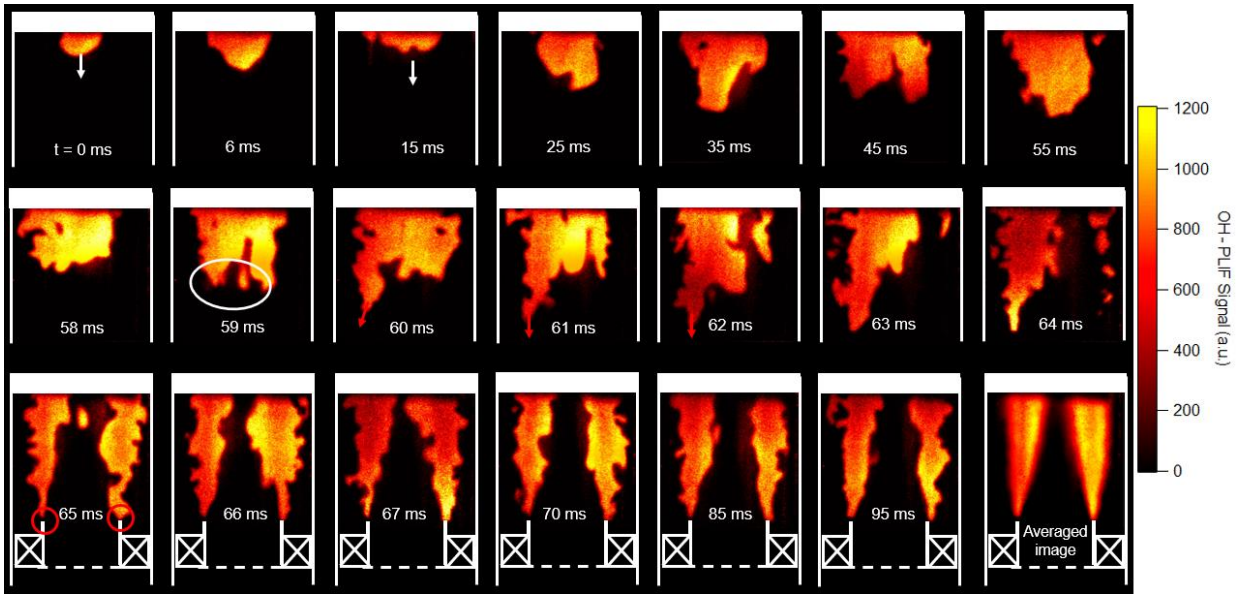

Figure 8: Sequence of single-laser shot OH-PLIF images showing temporal evolution of flame flashback events inside the pre-mixer tube for 60%H_2/40%CH_4-air flame at V = 7.5 m/s. Several single-laser-shot OH-PLIF images were acquired visualizing the anchored flame and 200 such individual frames were averaged during post-processing and is depicted in bottom right corner.

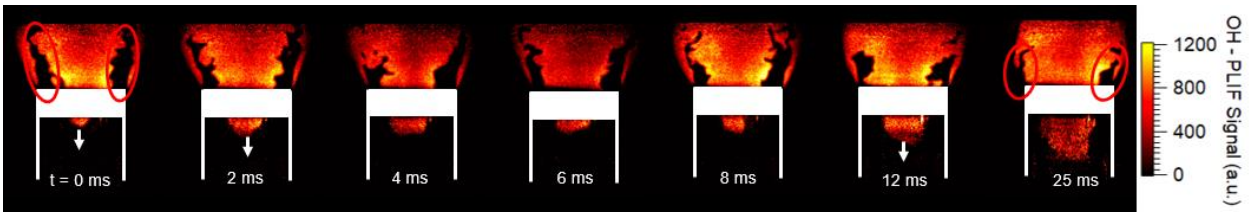

Figure 9: Initial phase of flame flashback for 70%H_2/30%CH_4-air flame at V = 10 m/s.

2. Effect of Fuel Compositions

Figure 10a shows the dependence of flashback equivalence ratio (ϕ_{FB}) on the proportion of X_{H_2} (60% to 90%) in reactant mixtures for three different V (5, 7.5, and 10 m/s). It is observed that at a constant V, ϕ_{FB} decreases linearly with an increase in X_{H_2} in the reactant mixture. As X_{H_2} increases in the H_2/CH_4-air mixture, the overall flame speed of the reactant mixture increases as mentioned earlier in Fig. 4b [24-26], and the flame flashback is more likely to occur. This statement is further evidenced by the decrease in L as X_{H_2} increases, indicated in Fig. 4a. As the V of the reactant mixture increases (keeping constant X_{H_2}), the flashback resistance of the burner system increases as the local fuel velocity grows large relative to the flame speed of the mixture. The dependence of ϕ_{FB} on the velocity at constant X_{H_2} was found to be linear as indicated in Fig. 10b. The error bar for the V of 7.5 m/s for 70%H_2/30%CH_4-air flame represents a 2-sigma standard deviation of ϕ_{FB} obtained from six different experimental tests.

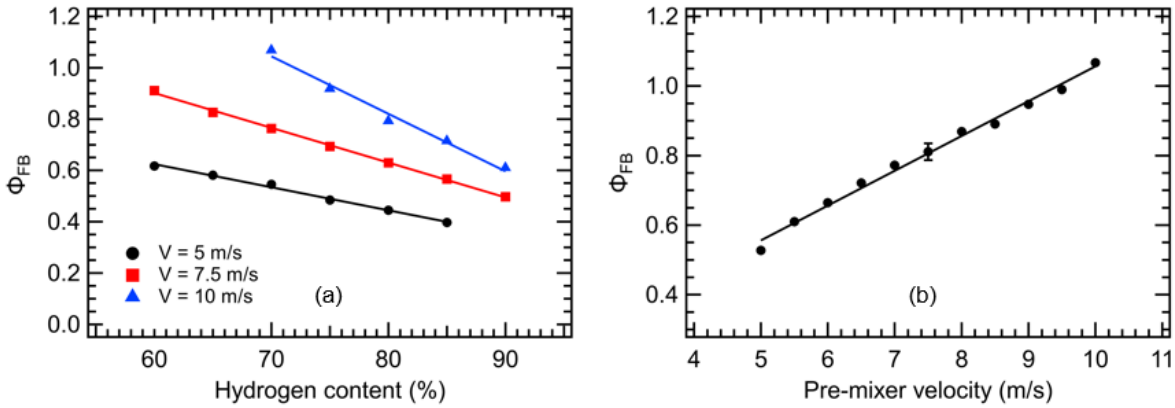

Figure 10: Dependence of ϕ_{FB} upon (a) X_{H_2} for three different Vs (5, 7.5, and 10 m/s) (b) V for 70%H_2/30%CH_4-air flame at reactants temperature 300 K and pressure 1 atm.

3. Variation of Swirler Design Parameters

Figure 11a shows the dependence of ϕ_{FB} on X_{H_2} for three different center-body hole diameters of 1.08, 1.12, and 1.16 mm creating blockage ratios (BR) of 0.783, 0.767, and 0.750 respectively. The swirl vane angle was kept constant at 33°. An increase in perforated plate hole diameter decreases the BR which increases the flow via the center-body and the burner system becomes less flashback prone, as depicted in Fig. 11a. In other words, reducing the axial mass flow rate via center-body (by increasing BR), results in flame flashback. Another interesting observation is on the slope of the flashback lines which shows a greater negative slope with increasing d (or decreasing BR). This means for the same amount of increase in X_{H_2}, the decrease in ϕ_{FB} is greater for a higher hole diameter (or a lower BR). No flashback was observed at lower X_{H_2} for d = 1.16 mm at V = 7.5 m/s even when flame ϕ is ramped to stoichiometric. The error bars shown for a few data points represent a 2-sigma standard deviation of ϕ_{FB} obtained from five different experimental tests. Figure 11b shows the dependence of ϕ_{FB} on X_{H_2} for two different swirl vane angles – 26° and 33° represented by black circle and blue triangles respectively. The center-body hole diameter was kept constant at 1.16 mm, creating a constant BR of 0.750. An increase in α increases the flashback resistance of the burner system at V =

7.5 m/s, as depicted in Fig. 11b. This could be because the increasing swirling angle creates a stronger swirl flow which promotes rapid divergence near the burner exit allowing better flame stabilization. The slope of the flashback lines for $\alpha = 33°$ shows a greater negative slope when compared to flashback lines for $\alpha = 26°$. The error bar represents a 2-sigma standard deviation of ϕ_{FB} obtained from five different experimental tests.

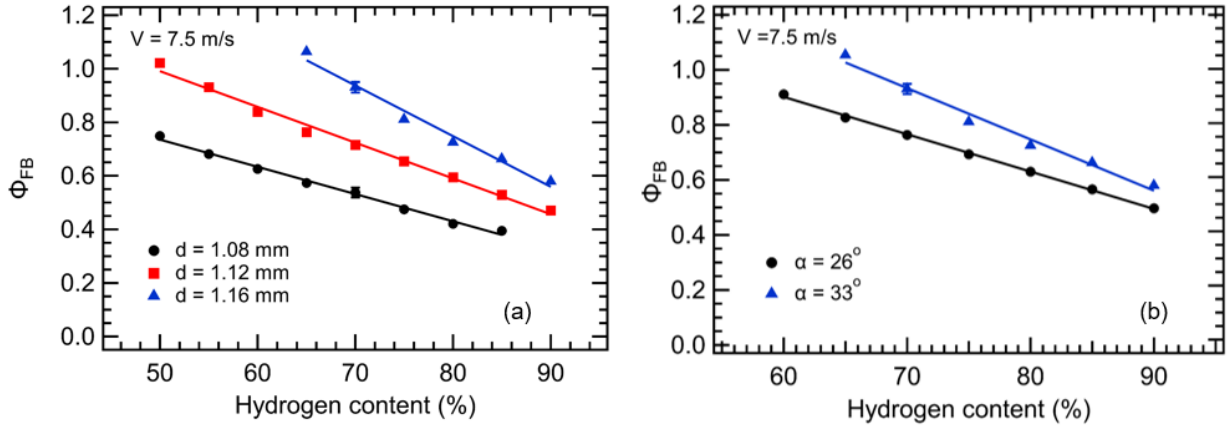

Figure 11: ϕ_{FB} as a function of X_{H_2} at V = 7.5 m/s for (a) three different perforated plate hole diameters, (b) two different swirler vane angles.

CONCLUSIONS

In this study, a ns-pulsed OH-PLIF diagnostic technique was applied to investigate the fundamentals of hydrogen-rich stable flames and flashback processes in a premixed LSB configuration at atmospheric temperature and pressure conditions. The inlet fuel-air mixtures were varied systematically with respect to ϕ and X_{H_2} in a hydrogen-methane mixture (50%–90% H_2 by mole), and pre-mixer velocities and the experiments were performed on a burner modified to provide optical access to the premixing section. Swirlers with two different turning angles of 26^o and 33^o and three different perforated plate hole diameters of 1.08, 1.12 and 1.16 mm with measured swirl numbers varying from 0.43 to 0.49 were used to investigate the LSB performance. Flame ϕ at flashback showed an expected linearly increasing trend with increasing V and decreasing X_{H_2} and the conclusions drawn aligned well with detailed lift-off length investigations. For identical inlet conditions, flashback propensity decreases with increasing hole diameter in the perforated plate and increasing swirler vane angle.

High-speed OH-PLIF images revealed that lifted flames were first observed at low ϕ/ X_{H_2} condition which were attached to burner rim with an increase in ϕ/ X_{H_2}. Additional increase in ϕ/X_{H_2} triggered flame flashback into the pre-mixing section. Flashback occurred when burning began in the outer shear layer and the leading flame brush propagated into the nozzle. The inner shear layer between swirled and unswirled flows above the center channel wall assisted the upstream flame propagation inside the pre-mixer tube. It was found that post-flashback flame stabilization occurred on the rim of center-body between swirling and non-swirling regions forming a conical flame. Based on these findings and insights from the LSB performance, specific guidelines and recommendations on geometry modifications to the LSB have been provided. The insights gained by these studies could be augmented by computational fluid dynamics simulations or simultaneous velocimetry and PLIF diagnostics which are the subject of future study.

ACKNOWLEDGMENTS

This work was performed in support of the U.S. Department of Energy's (DOE) Fossil Energy and Carbon Management's Hydrogen Combustion Research Program and executed through the National Energy Technology Laboratory (NETL) Research & Innovation Center's Turbines Field Work Proposal. The authors acknowledge the contribution of Matthew Searle for his valuable input during burner design, modification, and operation.

DISCLAIMER

This project is funded by the United States Department of Energy, National Energy Technology Laboratory, in part, through a site support contract. Neither the United States Government nor any agency thereof, nor any of their employees, nor the support contractor, nor any of their employees, makes any warranty, express or implied, or assumes any legal liability or responsibility for the accuracy, completeness, or usefulness of any information, apparatus, product, or process disclosed, or represents that its use would not infringe privately owned rights. Reference herein to any specific commercial product, process, or service by trade name, trademark, manufacturer, or otherwise does not necessarily constitute or imply its endorsement, recommendation, or favoring by the United States Government or any agency thereof. The views and opinions of authors expressed herein do not necessarily state or reflect those of the United States Government or any agency thereof.

REFERENCES

1. Chapman, A., Itaoka, K., Farabi-Asl, H., Fujii, Y., and Nakahara, M. "Societal penetration of hydrogen into the future energy system: Impacts of policy, technology and carbon targets," *International Journal of Hydrogen Energy* Vol. 45, No. 7, 2020, pp. 3883-3898.
doi: https://doi.org/10.1016/j.ijhydene.2019.12.112
2. Cecere, D., Giacomazzi, E., and Ingenito, A. "A review on hydrogen industrial aerospace applications," *International Journal of Hydrogen Energy* Vol. 39, No. 20, 2014, pp. 10731-10747.
doi: https://doi.org/10.1016/j.ijhydene.2014.04.126
3. Ball, M., and Wietschel, M. "The future of hydrogen – opportunities and challenges," *International Journal of Hydrogen Energy* Vol. 34, No. 2, 2009, pp. 615-627.
doi: https://doi.org/10.1016/j.ijhydene.2008.11.014
4. Krishnan Unni, J., Govindappa, P., and Das, L. M. "Development of hydrogen fuelled transport engine and field tests on vehicles," *International Journal of Hydrogen Energy* Vol. 42, No. 1, 2017, pp. 643-651.
doi: https://doi.org/10.1016/j.ijhydene.2016.09.107
5. Verhelst, S., and Wallner, T. "Hydrogen-fueled internal combustion engines," *Progress in Energy and Combustion Science* Vol. 35, No. 6, 2009, pp. 490-527.
doi: https://doi.org/10.1016/j.pecs.2009.08.001
6. Xiao, Y., Cao, Z., and Wang, C. "Flame stability limits of premixed low-swirl combustion," *Advances in Mechanical Engineering* Vol. 10, No. 9, 2018, p. 1687814018790878.
doi: https://doi.org/10.1177/1687814018790878
7. Cheng, R. K. "Velocity and scalar characteristics of premixed turbulent flames stabilized by weak swirl," *Combustion and Flame* Vol. 101, No. 1, 1995, pp. 1-14.
doi: https://doi.org/10.1016/0010-2180(94)00196-Y
8. Cheng, R. K. "Low Swirl Combustion," *The Gas Turbine Handbook*. U.S. Department of Energy, National Energy Technology Laboratory, 2006, pp. 241 - 254.
9. Searle, M., and Strakey, P. "Flashback of Hydrogen-Methane Mistures in a Fixed-vane, Low-swirl Burner at Atmospheric Pressure," *Proceedings of ASME Turbo Expo 2023*. Boston, Massachusetts, June 26-30, 2023.
10. Luque, J., and Crosley, D. R. "LIFBASE: Database and spectral simulation program (version 1.5)," *SRI international report MP* Vol. 99, No. 009, 1999.
11. Lawn, C. J. "Lifted flames on fuel jets in co-flowing air," *Progress in Energy and Combustion Science* Vol. 35, No. 1, 2009, pp. 1-30.
doi: https://doi.org/10.1016/j.pecs.2008.06.003
12. Hwang, G. J., Jeon, D. S., and Kim, N. I. "Stabilization criteria of laminar lifted flames in a non-premixed jet through experiments at elevated pressures," *Fuel* Vol. 314, 2022, p. 122797.
doi: https://doi.org/10.1016/j.fuel.2021.122797
13. Liu, G., and Wu, Y. "Lift-off height model of hydrogen autoignited flame in turbulent hot air coflow," *International Journal of Hydrogen Energy*, 2023.
doi: https://doi.org/10.1016/j.ijhydene.2023.08.099
14. Lyons, K. M. "Toward an understanding of the stabilization mechanisms of lifted turbulent jet flames: Experiments," *Progress in Energy and Combustion Science* Vol. 33, No. 2, 2007, pp. 211-231.
doi: https://doi.org/10.1016/j.pecs.2006.11.001
15. Koyama, M., and Tachibana, S. "Technical applicability of low-swirl fuel nozzle for liquid-fueled industrial gas turbine combustor," *Fuel* Vol. 107, 2013, pp. 766-776.

doi: https://doi.org/10.1016/j.fuel.2013.01.038
16. Cabra, R., Myhrvold, T., Chen, J. Y., Dibble, R. W., Karpetis, A. N., and Barlow, R. S. "Simultaneous laser raman-rayleigh-lif measurements and numerical modeling results of a lifted turbulent H2/N2 jet flame in a vitiated coflow," *Proceedings of the Combustion Institute* Vol. 29, No. 2, 2002, pp. 1881-1888.
doi: https://doi.org/10.1016/S1540-7489(02)80228-0
17. Cabra, R., Chen, J. Y., Dibble, R. W., Karpetis, A. N., and Barlow, R. S. "Lifted methane–air jet flames in a vitiated coflow," *Combustion and Flame* Vol. 143, No. 4, 2005, pp. 491-506.
doi: https://doi.org/10.1016/j.combustflame.2005.08.019
18. T, G. "Lift-off Heights and Visible Lengths of Vertical Turbulent Jet Diffusion Flames in Still Air," *Combustion Science and Technology* Vol. 41, No. 1-2, 1984, pp. 17-29.
doi: 10.1080/00102208408923819
19. Yang, L., Weng, W., Zhu, Y., He, Y., Wang, Z., and Li, Z. "Investigation of Hydrogen Content and Dilution Effect on Syngas/Air Premixed Turbulent Flame Using OH Planar Laser-Induced Fluorescence," *Processes* Vol. 9, No. 11, 2021, p. 1894.
doi: https://doi.org/10.3390/pr9111894
20. Cheng, R. K., Littlejohn, D., Strakey, P. A., and Sidwell, T. "Laboratory investigations of a low-swirl injector with H2 and CH4 at gas turbine conditions," *Proceedings of the Combustion Institute* Vol. 32, No. 2, 2009, pp. 3001-3009.
doi: https://doi.org/10.1016/j.proci.2008.06.141
21. Pitsch, H. "Enabling Advanced Modeling and Simulations for Fuel-Flexible Combustors." National Energy Technology Laboratory, U.S. Department of Energy, 2010.
22. Darshan, R. "CFD Study on Flame Flashback in Low Swirl Premixed Burners." Vol. Master of Science, Delft University of Technology, 2022.
23. Therkelsen, P. L., Littlejohn, D., and Cheng, R. K. "Parametric Study of Low-Swirl Injector Geometry on its Operability," *ASME Turbo Expo 2012: Turbine Technical Conference and Exposition*. Vol. Volume 2: Combustion, Fuels and Emissions, Parts A and B, 2012, pp. 309-318.
24. Ilbas, M., Crayford, A. P., Yılmaz, İ., Bowen, P. J., and Syred, N. "Laminar-burning velocities of hydrogen–air and hydrogen–methane–air mixtures: An experimental study," *International Journal of Hydrogen Energy* Vol. 31, No. 12, 2006, pp. 1768-1779.
doi: https://doi.org/10.1016/j.ijhydene.2005.12.007
25. "The path towards a zero-carbon gas turbine," *Hydrogen Gas Turbines*. European Turbine Network (ETN) Global, Brussels, Belgium, 2020.
26. Goldmeer, J. "Fuel flexible gas turbines as enablers for a low or reduced carbon energy ecosystem," *Electrify Europe: Vienna, Austria*, 2018.